

# Hybrid Electric Vehicle Characterization Using Generalized Notion of Power

N. Al-Aawar<sup>1,2</sup> and A. A. Arkadan<sup>1,2</sup>

<sup>1</sup>Rafik Hariri University, Mechref, Damour, 2010, Lebanon

<sup>2</sup>Marquette University, Milwaukee, WI, 53203, USA  
a.a.arkadan@marquette.edu

**Abstract**—This paper presents a novel mathematical model based on the generalized notion of power (GNP) to accurately predict the performance characteristics of hybrid electric vehicles (HEVs). The uniqueness of this technique is the ability to represent both internal combustion engine and electrical propulsion machines in one system of state space equations. Thus, it allows proper characterization and control of the interaction of both systems by taking into account large and small load disturbances and the irreversibility of entropy generation by the internal combustion engine. The superiority of the proposed model is demonstrated by applying it to a prototype HEV configuration and by comparison to readily available benchmark data.

**Index Terms** - Electric machines, hybrid electric vehicles, internal combustion engines, magneto-statics, and mathematical models.

## Nomenclature

HEV	Hybrid Electric Vehicle
EMG	Electric Motor Generator
ICE	Internal Combustion Engine
I	EMG Windings Current
R	EMG Windings Resistance
L	EMG windings Inductance
$\omega$	Electric angular speed
$\theta$	Rotor position
$U_V$	EMG Windings Voltage
J	Moment of inertia of the EMG rotor
$T_{dev}$	Developed torque of the EMG
$T_{load}$	Load torque
$q_E$	Flow variable at electric port

$e_E$	Effort variable at electric port
$q_M$	Flow variable at mechanical port
$e_M$	Effort variable at mechanical port
$U_i$	Internal energy
$S_i$	Entropy
$V_i$	Volume
$T_i$	Temperature
$P_i$	Pressure
i	Index the thermodynamic state
m	Mass of the air
$C_v$	Specific heat at constant volume of the air
$R_g$	Ideal gas constant.

## I. INTRODUCTION

The demand for more environmentally friendly and fuel efficient vehicles has increased in response to growing concerns for clean environment and energy savings. In this context, the hybrid electric vehicle (HEV) has emerged as a viable solution to meet these requirements. There are different powertrain configurations in HEVs. However, all involve integrating several power sources, mainly internal combustion engine, ICE, and electrical motor generator (EMG) unit in the vehicle to improve its performance. The performance of HEVs depends on the design of the powertrain system and the integration of the power sources. Accordingly, accurate performance characterization, including the interaction of mechanical and electrical components, is essential to optimize the design of the powertrain and thus the performance of the HEV. However, this proves to be very challenging because of the dynamic nature of the interactions among various components of HEV [1, 2]. In [1] an integrated

team artificial intelligence electromagnetic, T-AI-EM environment was developed to accurately determine the performance characteristics of synchronous reluctance machines (SynRM) with axially laminated anisotropic rotor configurations for powertrain usage. In another work, the PLC network was used to improve the communication inside the hybrid electric vehicle [3]. Much of the earlier works involved the use of finite state machine (FSM) to model the interaction between the ICE and EMG. It simulates an offline control strategy that manages the developed power to balance the load power for a given state of operation of the HEV [2, 4, 5]. The drawback of such approaches is its inability to capture the effect of small load disturbances. Thus, the HEV will not operate at near optimum conditions. This paper presents a novel technique that models both EMG and ICE into one system of state space equations. Accordingly, it enables the use of real time control strategies that could adaptively change the degree of hybridization of the vehicle in response to large and small load disturbances to achieve near optimum performance conditions. In the following, we present the conventional and the proposed GNP models. The models are next applied to a prototype HEV configuration and the results are compared to available benchmark data for validation.

## II. THE CONVENTIONAL MODEL

The conventional model of HEV starts by adopting certain configuration of connecting the ICE and the EMG, such as the series, parallel or split power configuration, Fig. 1. Next, each of the ICE and EMG is modeled as a standalone component and are integrated by using a power balance equation to simulate the propulsion of the vehicle in accordance with the status of the operation of the vehicle [6]. One way is to model the EMG by nonlinear state space equations as follows,

$$\dot{I} = L^{-1} \left( R + \omega \frac{\partial L}{\partial \theta} \right) I + L^{-1} U_v \quad (1)$$

$$\dot{\omega} = \frac{T_{dev} - T_{load}}{J} \quad (2)$$

$$T_{dev} = I^T \omega \frac{\partial L}{\partial \theta} I \quad (3)$$

where,  $I$  is the current,  $R$  is the resistance,  $L$  is the inductance,  $\omega$  is the electric angular speed,  $\theta$  is the rotor position,  $U_v$  is the voltage,  $J$  is the moment of inertia of the rotor,  $T_{dev}$  is the EMG developed torque, and  $T_{load}$  is the load torque. The complex structure and the nonlinear nature of the magnetic material of the EMG system cause the inductances of the electric machine to be function of the rotor position and load current. Thus, the family of curves technique [7] is adopted and nonlinear magnetic field solutions are used to represent each inductance by a set of curves function of rotor position and current load condition, Fig. 2. The state space model is used to compute the winding currents and the developed torque for the given input voltages and load torque [7, 8]. A computational electromagnetic (EM) module is used to model the EMG. This module accounts for the non-linearity of the EMG magnetic material, space harmonics due to its geometry, as well as the time harmonics resulting from switching electronics in the load. This module utilizes an indirectly coupled FE-SS approach to compute sets of winding inductances as function of load and rotor position. The method is outlined in Fig. 2 where for each rotor position the EM solutions corresponding to a range of the excitation currents are computed. These solutions are used to compute the device windings inductances. Next, the rotor is moved an increment,  $\Delta\theta$ , to a new position and the task is repeated to cover a complete AC cycle. In this work,  $\Delta\theta$  was chosen at a value that moves the rotor to positions alternatively between “middle of slot” and “middle of tooth” of the stator to account for the slotting effects. Once a full electrical cycle of the rotor motion is completed, a set of family of curves is obtained [7]. A sample family of curves, for the stator winding mutual inductance  $L_{ab}$  is shown in Fig. 3, which is function of load and rotor position. These sets of curves are integrated with the state space model in order to accurately predict the performance characteristics of the EMG.

As for the ICE model, the engine efficiency map of Fig. 4 is used. Here, the ICE is assumed to operate at the optimum operating line (OOL), which is a sequence of intersections of the constant engine power lines with the peak efficiency contours [9]. The EMG and ICE combine to develop the torque required to propel

the vehicle. The finite state machine of Fig. 5 is used to define the state of operation of the HEV powertrain. The HEV state of operation like starting, cruising, breaking, Fig. 5, decides the degree of hybridization of the vehicle. The degree of hybridization is defined as the power developed by the EMG over the required load power. The state of operation of the HEV can be based on a load-following strategy or an on/off strategy. In the case of a load-following strategy, the power from the power propulsion unit (PPU) is closely related to the power demand from the chassis. If the strategy is the on/off type, the power from power propulsion unit is related to the state of charge (SOC) of the batteries. At some specific SOC, the PPU is turned on or off. In practice, a combination of the strategies might be the most appropriate choice [9]. The main principle is that when a specific state is active an output related to that state would be generated. An example of the generated output for “starting state is: Motor\_enable=1, Generator\_enable=1 and Ice\_enable=0; in this mode the HEV works as an electric vehicle. A state of operation of the vehicle is activated based on the “throttle” and “breaking” positions. A state will remain active till a change occurs, such as change of vehicle speed and or pedal position; then another state will become active, Fig. 5. As can be appreciated, this type of operation cannot be used to adaptively change the degree of hybridization when small disturbances occur in the load. Therefore, the HEV performance will be far from being optimum.

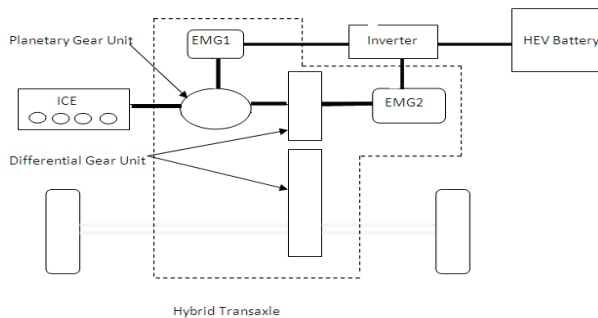


Fig. 1. Toyota prius split power configuration.

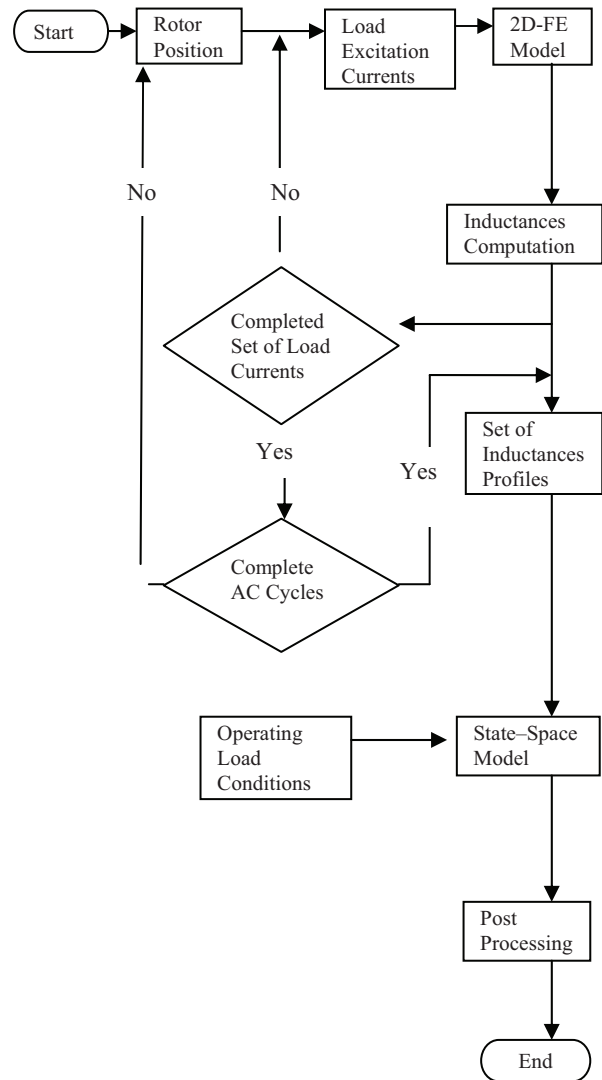


Fig. 2. Inductance family of curves computation.

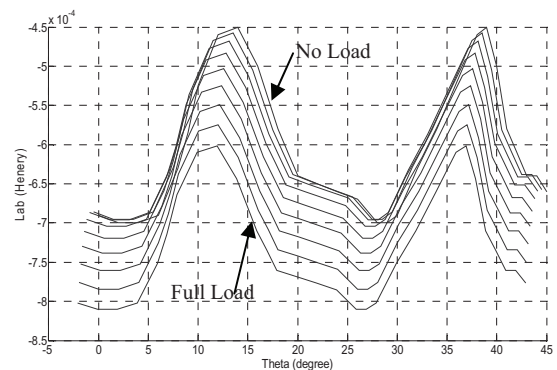


Fig. 3. Family of curves of mutual inductance  $L_{ab}$ .

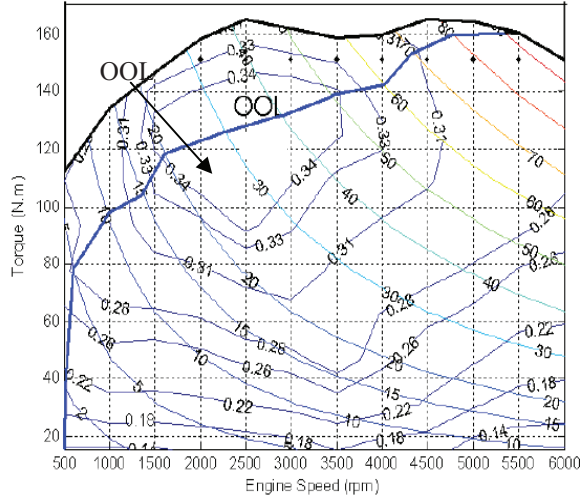


Fig. 4. Engine efficiency map.

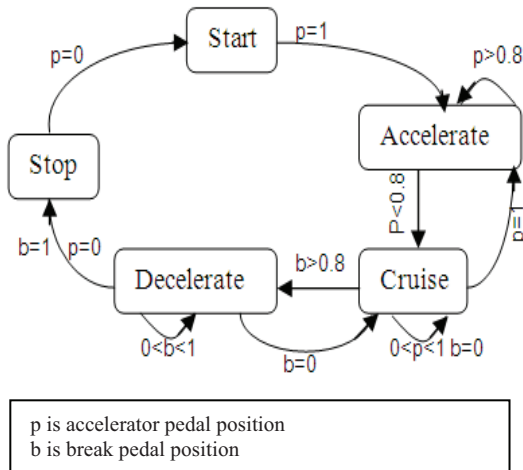


Fig. 5. Finite state machine of HEV.

### III. GENERALIZED NOTION OF POWER MODEL

The aim of this work is to develop an accurate model that precisely predicts the performance of the HEV for all types of driving cycles including small road disturbances. The main principle is to develop a torque equal to a load torque to propel the car while maintaining optimum performance of the ICE and SOC higher than 20 % to protect the batteries [8]. The generalized notion of power [10] is used in this work to unify the notation for both EMG and ICE systems so it can be modeled in one system of state space equations. The GNP is implemented as the vector multiplication of effort variable  $e$  and the generalized displacement

vector  $q$  to arrive to the power and thus the torque. The adoption of the GNP model facilitates the use of real time controller such as the proportional-integral-derivative (PID) controller to manage the interactions between the EMG and the ICE at near optimum performance conditions. The details of developing the GNP model for the HEV are given below.

#### A. The EMG model

An electric motor generator (EMG), according to its structure, can be represented as a dual-port system. The first port is the electrical winding and the second is the mechanical shaft. The machine dynamics are described by two power variables at each port. Using the generalized notion of power representation, the current in the EMG system is treated as a displacement variable,  $q$ , and the voltage as an effort variable,  $e$ . Moreover, the rotor angular velocity and the developed torque are the displacement and effort, respectively, at the mechanical port, Fig. 6. Using the GNP representation in equations (1) to (3) above will result in equations (4) to (6),

$$\dot{q}_E = L^{-1} \left( R + q_M \frac{\partial L}{\partial q_M} \right) q_E + L^{-1} e_E \quad (4)$$

$$\dot{q}_M = \frac{e_M - e_{load}}{J}, \quad (5)$$

$$e_M = q_E^T q_M \left( \frac{\partial L}{\partial \theta} \right) q_E. \quad (6)$$

where  $L$  is the inductance matrix and  $e_M$  is the effort of the mechanical port. The inductance matrix,  $L$ , of equation (4) can be calculated from nonlinear magnetic field solutions or test data and represented by the family of curves approach outlined above in Fig. 2. Accordingly, it accounts for the nonlinearity of the magnetic material and the complex structure of the EMG.

#### B. The ICE Model

The ICE is a thermodynamic device that generates mechanical work and heat based on the first and second laws of thermodynamics as shown in the P-V and T-S diagrams of Fig. 7. The Otto cycle consists of adiabatic compression, heat addition at constant volume, adiabatic expansion, and rejection of heat at constant volume. In the case of a four-stroke Otto cycle, technically there

are two additional processes: one for the exhaust of waste heat and combustion products (by isobaric compression) and one for the intake of cool oxygen-rich air (by isobaric expansion); however, these are often omitted in a simplified analysis. The Otto cycle is summarized by the following process [9]:

- Process 0-1 represents an isentropic compression of the working gas as the piston moves up the cylinder.
- Process 1-2 is a constant-volume ignition of the air fuel mixture.
- Process 2-3 is an isentropic expansion while the piston is pushed down the cylinder. This phase is known as the power stroke.
- Process 3-0 is the rejection of the exhaust gas out of the cylinder at constant volume.

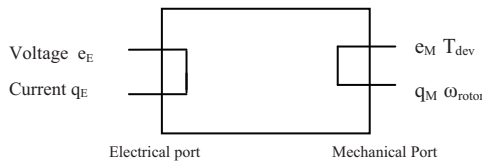


Fig. 6. Schematic of EMG using GNP notation.

Hence, the internal energy  $U(S,V)$  is a scalar potential function defined in the space of displacements spanned by  $S$  (entropy) and  $V$ , volume. The efforts in the two domains (thermal and mechanical) may be defined as  $e = [T,P]^T$ , where  $T$  is the temperature and  $P$  is the pressure. For simplicity, the equations are linearized about a nominal operating point defined by  $S_0$  and  $V_0$  where,

$$\begin{aligned} \delta S &= S - S_0 \\ \delta V &= V - V_0, \\ \delta T &= T - T_0(S_0, V_0), \\ \delta P &= P - P_0(S_0, V_0). \end{aligned} \tag{7}$$

Taylor series expansion is utilized as follows:  
 $\delta T = \partial T/\partial S|_{S_0V_0} \delta S + \partial T/\partial V|_{S_0V_0} \delta V +$  higher order terms;  
 $\delta P = \partial P/\partial S|_{S_0V_0} \delta S + \partial P/\partial V|_{S_0V_0} \delta V +$  higher order terms. Neglecting the higher-order terms and dropping the  $\delta$  prefix for convenience; a linearized model of the ICE is obtained as shown in the equation below,

$$\begin{aligned} T &\approx AS - BV \\ P &\approx BS - CV, \end{aligned} \tag{8}$$

where  $A$ ,  $B$ , and  $C$  are positive constants defined by,

$$\begin{aligned} A &= \partial T/\partial S = T_0/mC_v \\ B &= \partial P/\partial S = -\partial T/\partial V = P_0/mC_v, \\ C &= -\partial P/\partial V = \left(\frac{P_0}{V_0}\right)\left(\frac{R_g}{C_v} + 1\right). \end{aligned} \tag{9}$$

The symbol  $m$  is the mass of the air,  $C_v$  is the specific heat at constant volume of the air, and  $R_g$  is ideal gas constant. The Internal energy corresponding to this linearized approximation is a quadratic form in  $S$  and  $V$  and is given by:

$$U = 1/2 A S^2 - B SV + 1/2 C V^2. \tag{10}$$

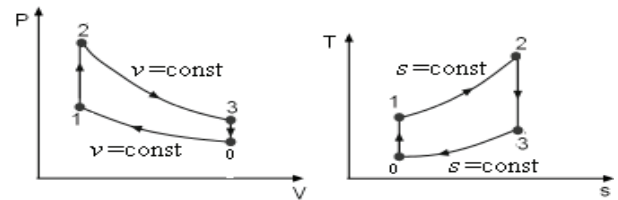


Fig. 7. P-V and T-S diagram of internal combustion engine.

The Otto cycle summarized in Fig. 7 is described as follows, STATE 0: everything at thermal equilibrium ( $S_0, V_0$ ),

$$\begin{aligned} T_0 &= AS_0 - BV_0 \\ P_0 &= BS_0 - CV_0, \\ U_0 &= 1/2AS_0^2 - BS_0V_0 + 1/2CV_0^2. \end{aligned} \tag{11}$$

The transition between state 0 to state 1 is represented by an adiabatic compression of the working gas as seen in Fig. 7. This compression occurs at constant entropy and at a volume change,  $-\Delta V$ . STATE 1: is represented by the variables ( $S_0$ ) and ( $V_0 - \Delta V$ ) thus temperature and pressure increases as follows,

$$\begin{aligned} T1 &= AS_0 - B(V_0 - \Delta V) = T_0 + B\Delta V \\ P1 &= BS_0 - C(V_0 - \Delta V) = P_0 + C\Delta V. \end{aligned} \tag{12}$$

The energy generated is given by the following equation,

$$U1 = 1/2AS_0^2 - BS_0(V_0 - \Delta V) + 1/2 C(V_0 - \Delta V)^2 \tag{13}$$

The internal energy increases by an amount equal to the work done on the gas and is given by,

$$U1 - U_0 = P_0\Delta V + 1/2C\Delta V^2. \tag{14}$$

Each of these transition processes of Fig. 6 can be developed in a similar way as from state 0 to state 1 and they can be represented in state space format as follows,

$$\begin{bmatrix} \delta T \\ \delta P \end{bmatrix} = \begin{bmatrix} \frac{\partial T}{\partial S} & \frac{\partial T}{\partial(-V)} \\ \frac{\partial P}{\partial S} & \frac{\partial P}{\partial(-V)} \end{bmatrix} \begin{bmatrix} \delta S \\ \delta(-V) \end{bmatrix}. \quad (15)$$

The torque developed by the ICE as result of the above analysis computed for all the Otto cycle is given as follows,

$$e_{\text{eng}} = A \Delta S^2 / \omega_{\text{eng}} \quad (16)$$

where  $\omega_{\text{eng}}$  is the angular rotation of the crank shaft of the ICE.

### C. Integration of EMG and ICE

The key objective of this work is to develop a GNP based model of the HEV powertrain. This model can be used with a real time control strategy to adaptively change the degree of hybridization of the vehicle in response to large and small load disturbances and to achieve near optimum performance. This is demonstrated by simulating a PID real time control strategy that manages the interaction between the ICE and the EMG of the HEV powertrain system. The strategy is summarized in Fig. 8. In this strategy, the load torque is computed from the driving cycle. Also, an initial voltage and initial pedal position are selected. The pedal position is used to iteratively determine the entropy and the displaced volume of the ICE and therefore the torque. The selected EMG voltage is used to initiate an iterative process between the state space model and family of curves to accurately calculate the winding currents and the EMG developed torque. Next the total developed torque ( $T_{\text{dev}} + T_{\text{eng}} = e_M + e_{\text{eng}}$ ) and the degree of hybridization ( $T_{\text{dev}} / (T_{\text{dev}} + T_{\text{eng}})$ ) are computed. This developed torque is used in the kinematic and kinetic equations of the HEV to determine the load torque and actual driving cycle. This driving cycle is checked with the reference driving cycle. The controller will continue on changing the initial dc bus voltage and the pedal position till both driving cycles match (within 5 % error).

## IV. APPLICATION AND RESULTS

The split power configuration of Fig. 1 for a prototype Toyota Prius was modeled using both conventional and proposed GNP models presented in this paper. As shown in Fig. 1, this configuration consists of two EMGs of the internal permanent magnet (IPM) type.

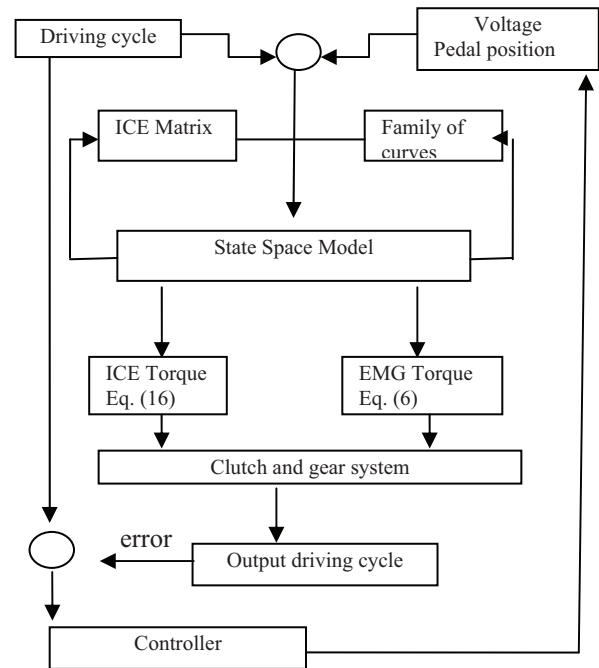


Fig. 8. Real time control strategy of HEV.

These two EMGs are rated at 28 kW and 50 kW, respectively. The bank of batteries consists of 168 cells of NINH type that is rated at 21 kW [6]. The ICE is a 4-cylinder aluminum double overhead cam (DOHC) 16-valve VVT with displacement of 1.5 L [2]. The vehicle is tested for urban driving cycle, UDC. The results presented in this paper are generated using the conventional model and the novel GNP model proposed in this work for the same operating conditions of references [2, 6]. The results are shown in Fig. 9 to Fig. 12 and are compared to available benchmark data [2, 6]. Figures 9 and 10 show the predicted load torque and SOC as computed by both models and compared to benchmark data. As can be appreciated from these results, the GNP model presented in this work better captures the effects of small load disturbances as compared to the conventional model. Also the GNP model results agree more with the benchmark data. In addition, Figs. 11 and 12 present a comparison between fuel consumption of the ICE as predicted by the GNP and conventional models, respectively. An inspection of these results reveals that the GNP model prediction of fuel consumption is closer to the benchmark data than that of the conventional model. It also reveals the superiority of the GNP model as it allows the use of real time PID

controller that adaptively changes the degree of hybridization by idling the ICE at very low engine rpm and activating the EMG. This translated into less fuel consumption, which is shown to be at 3.6 % for the urban drive cycle (UDC) simulated in this work as shown in Table I. In addition, Table I shows the values of two main performance indicators (fuel consumption and batteries SOC) as predicted by the GNP and conventional models and compared to readily available benchmark data. As can be appreciated from these results, the GNP model better captures the performance characteristics of the HEV powertrain system.

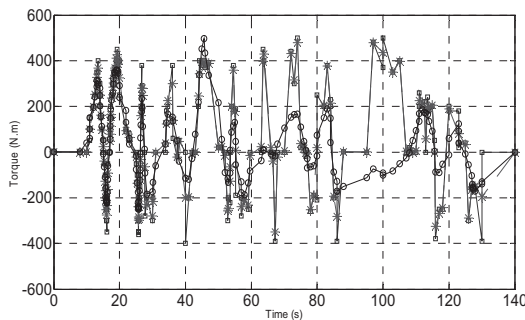


Fig. 9. Load torque versus time as computed by conventional (-o-), GNP(-\*-), and benchmark(-).

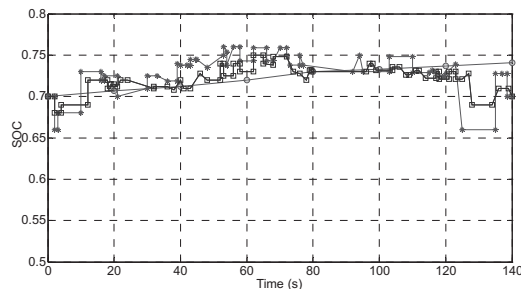


Fig. 10. SOC versus time and computed using conventional (-o-), GNP (-\*-), and Benchmark (-).

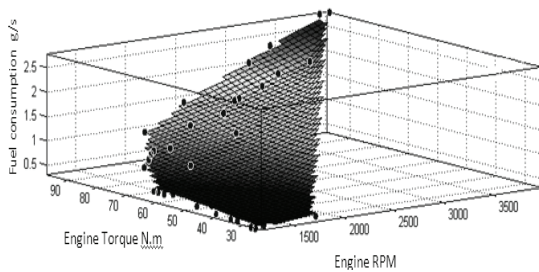


Fig. 11. Fuel consumption of ICE as predicted by the GNP model and compared to benchmark data (.).

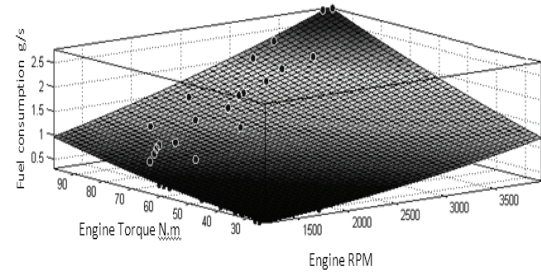


Fig. 12. Fuel consumption of ICE as predicted by the conventional model and compared to benchmark data (.).

Table I: Comparison of performance indicators as obtained from GNP and conventional models and benchmark data.

Description	Benchmark	GNP Model	Conventional Model
Fuel consumption	45 mpg	46.6 mpg	42.9 mpg
SOC at End of Cycle	0.74	0.7	0.7

### V. CONCLUSIONS

A novel mathematical model, based on the generalized notion of power to accurately predict the performance characteristics of hybrid electric vehicles, was presented. As was shown, the uniqueness of this technique is the ability to represent both internal combustion engine and electrical propulsion machines in one system of state space equations. Thus allowing proper characterization and control of the interaction of both systems by taking into account small load disturbances and irreversibility of the entropy generation by the internal combustion engine. The validity of this approach was shown by applying both GNP and conventional models to a split power configuration of an HEV powertrain system and by comparing the results to available benchmark data. The superiority of the GNP model was demonstrated as it allows the use of real time PID controller that adaptively changes the degree of hybridization of the powertrain system and as it can better capture the effects of small load disturbances.

### REFERENCES

[1] N. Al-Aawar, A. Hanbali and A. Arkadan, "Characterization and design optimization of ALA rotor synchronous reluctance motor drives for

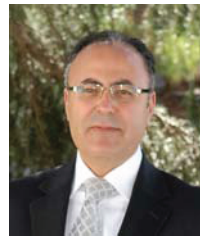
traction applications,” *22<sup>nd</sup> Annual Review of Progress in Applied Computational Electromagnetics (ACES)*, pp. 249-256, Florida, USA, March 2006.

- [2] USA DOE Plug-in Hybrid Electric Vehicle R&D Plan, 2007.
- [3] S. Barmada, M. Raugi, and M. Tucci, “Analysis of power line communications channels on board a fully electric vehicle,” *26<sup>th</sup> Annual Review of Progress in Applied Computational Electromagnetics (ACES)*, pp. 441-446, Tampere, Finland, April 2010.
- [4] A. Rousseau, P. Sharer, and F. Besnier, “Feasibility of reusable vehicle modeling: Application to hybrid vehicles,” *SAE World Congress*, Detroit, March 2004.
- [5] L. Boulon, A. Bouscayrol, D. Hissel, O. Page, and M.-C. Pera, “Inversion-based control of highly redundant military HEV,” *IEEE Transactions on Vehicular Technology*, vol. 62, no. 2, pp. 500-510, 2013.
- [6] N. Barcaro, N. Bianchi, and F. Magnussen, “PM motor for hybrid electric vehicle,” *The Open Fuels and Energy Science Journal*, pp. 135-141, 2009.
- [7] A. Arkadan, R. Heiden, and J. Defenbaugh, “Effects of forced power transfer on high speed generator-load system,” *IEEE Transactions on Energy Conversion*, vol. 11, no. 2, pp. 344-352, June 1996.
- [8] N. Al-Awar, T. Hijazi, and A. Arkadan, “Particle swarm optimization of coupled electromechanical systems,” *IEEE Transaction On Magnetics*, vol. 47, no. 5, pp. 1314-1317, 2011.
- [9] P. Curto-Risso, “Theoretical and simulated models for irreversible Otto cycle,” *IEEE Journal of Applied Physics*, vol. 104, no. 9, pp. 094911-094911-11, Nov. 2008.
- [10] J. Ginsberg, *Advanced Engineering Dynamics*, 2<sup>nd</sup> ed. Cambridge, UK: Cambridge University Press, ISBN: 9780521470216, 1995.



**Nizar Al-Awar** received his Bachelor of Engineering in Mechanical Engineering from American University of Beirut, Beirut Lebanon in 1994 and his Master degree from Marquette University in Electrical and Computer Engineering in 2003. He is currently completing his PhD in Electrical and Computer Engineering at Marquette University. During the period 2005 -2008 he worked in industry. In 2008, he joined the Department of Mechanical and

Mechatronics at Rafik Hariri University as a lecturer. Mr. Al-Awar authored and co-authored more than 20 technical papers in the archival literature as well as in National and International Conference records. In addition, he co-authored a white paper on assessment and solution to the problem facing electricity and water sector in Lebanon. Mr. Al-Awar received several awards for his achievements.



**A. A. Arkadan** received his Bachelor of Science degree from the University of Mississippi, Oxford, Mississippi in 1980, his Masters of Science degree from Virginia Tech, Blacksburg, Virginia in 1981 and his Ph.D. from Clarkson University, Potsdam, New York in 1988, all in Electrical Engineering. During the period 1981-1984 he worked in industry. In 1988, he joined the Department of Electrical and Computer Engineering at Marquette University, Milwaukee, Wisconsin, as an Assistant Professor and was later promoted to Associate Professor and Full Professor in 1993 and 1998, respectively. He has many years of teaching, curriculum development and research, as well as industrial and consulting experience. Currently, he is a Professor and President of Rafik Hariri University, in Mechref Lebanon. Dr. Arkadan is a Fellow of the Institute of Electrical and Electronics Engineers, IEEE. He authored and co-authored more than 100 technical papers in the archival literature as well as in National and International Conference records. In addition, he authored book chapters, numerous technical and project reports. Dr. Arkadan received several awards for excellence in research including several IEEE society awards. Dr. Arkadan is active in several IEEE and other international societies. Also he serves or served on the Editorial Boards of several International Conferences. In addition, Dr. Arkadan chaired several international conferences including the First IEEE International Electric Machines and Drives Conference, IEMDC, held in Milwaukee Wisconsin, May 1997, and the IEEE Conference on Electromagnetic Field Computations, CEFC, held in Chicago, Illinois, in May 2010. He is also the Chair of CEFC International Steering Committee.